Acta Mech 220, 331–348 (2011)
DOI 10.1007/s00707-011-0479-x

Hoang Chi Tran · Jaehong Lee

Determination of a unique configuration of free-form tensegrity structures

Received: 18 October 2010 / Published online: 3 April 2011

Abstract A numerical method is presented for form-finding of free-form tensegrity structures. The topology and an initial randomly generated force density vector are the required information in the present form-finding process. An approach of defining a unique configuration of free-form tensegrity structures by specifying an independent set of nodal coordinates is rigorously provided, which means that the geometrical and mechanical properties of the structure can be at least partly controlled by the proposed method. Several numerical examples are presented to demonstrate the efficiency and robustness in searching new self-equilibrium stable free-form configurations of tensegrity structures.

1 Introduction

Over the past few decades, tensegrity structures first proposed by Fuller [1] have attracted considerable attention in a wide diversity of fields including aerospace [2], architecture [3,4], civil engineering [5–7], biology [8–10], mathematics [11,12] and robotics [13,14]. They belong to a class of free-standing pre-stressed pin-jointed cable-strut system where contacts are allowed among the struts [15]. Their classification is presented as class 1 (where bars do not touch) and class 2 (where bars do connect to each other at a pivot) [16]. It is well known that a tensegrity structure has been considered as an appropriate model for capturing the mechanical behaviour of the cytoskeleton of living cells [8–10]. The cytoskeleton shown in Fig. 1 is a complex structure composed of three different polymer filaments: microfilaments (in tension), microtubules (in compression) and intermediate filaments (connecting microfilaments and microtubules to one another). However, the geometry and topology of the filament networks are so complex and free-form that current tensegrity models [17–19] cannot fit such configurations. Hence, there is still a demand to look for new methods allowing the design of complex and free-form tensegrity structures.

For the form-finding of regular tensegrities, there have been extensive researches in which analytical methods are suitable only for simple tensegrities with high symmetry [20–23]. As a pioneering work of numerical form-finding, the so-called force density method was proposed by Schek [24] for form-finding of tensile structures. Motro et al. [25] then presented the dynamic relaxation that has been reliably applied to tensile structures [26] and many other nonlinear problems. Recently, Masic et al. [27], Zhang and Ohsaki [28] and Estrada et al. [29] developed new numerical methods using the force density formulation. Pagitz and Mirats Tur [30] suggested a form-finding algorithm that is based on the finite element method. Most recently, Tran and Lee [31] proposed an advanced form-finding for tensegrity structures based only on the given topology and types

H. C. Tran · J. Lee (✉)
Department of Architectural Engineering, Sejong University, 98 Kunja Dong,
Kwangjin Ku, Seoul 143-747, Korea
E-mail: jhlee@sejong.ac.kr; chihoangkt@yahoo.com
Tel.: +82-2-3408-3287
Fax: +82-2-3408-3331

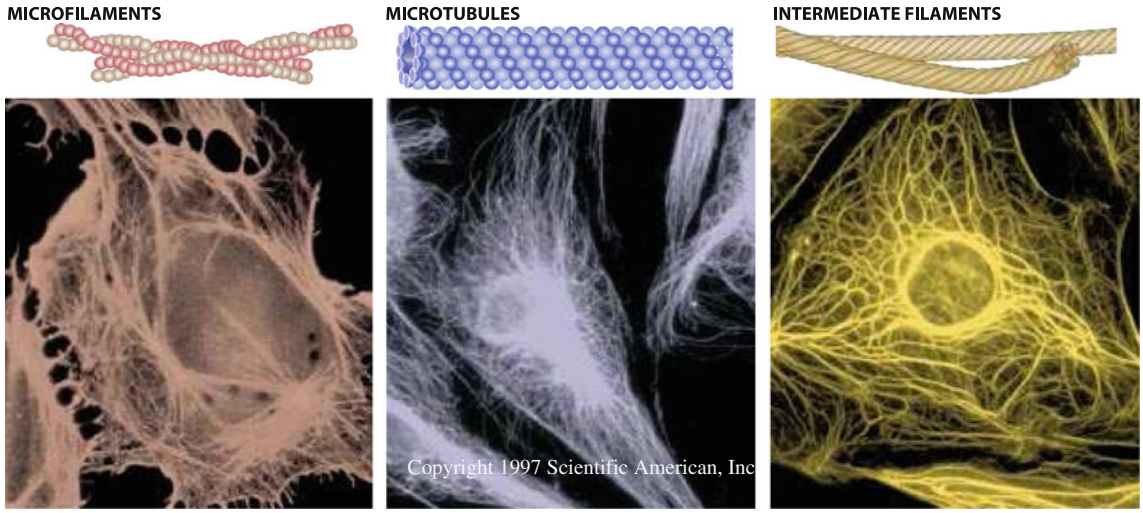

Fig. 1 Cytoskeleton polymer networks of a living cell [8]

of members, i.e., either tension or compression. A review of the existing methods for form-finding of regular tensegrity structures can be found in [32–34].

For irregular tensegrities, the form-finding problem is very difficult to be solved analytically, to authors' knowledge. So far, only a few numerical approaches have been proposed for this. Zhang et al. [35] and Baud et al. [36] employed the dynamic relaxation method for form-finding of nonregular tensegrities by modifying their corresponding regular ones. Micheletti et al. [37] used a marching procedure for finding stable placements of irregular tensegrities based on their given regular counterparts. Moreover, these two approaches are effective only for tensegrities with a small number of members. Recently, Rieffel et al. [38] introduced an evolutionary algorithm for producing large irregular tensegrity structures. Following their track, Xu and Luo [39] also proposed a genetic algorithm, but applied different optimization models from that in [38]. These methods are mainly based on the discrete optimization technique associated with the dynamic relaxation method for solving the irregular form-finding problem. However, in each iteration step of dynamic relaxation, all nodes are moved simultaneously with velocities calculated from unbalanced nodal forces. The solution may oscillate around some particular states of a structure. Consequently, the dynamic relaxation method can be ineffective when the number of nodes in the structure increases [34,39]. In most available form-finding methods for irregular tensegrities, initial nodal coordinates or member lengths and some initial member forces must be assumed known in advance in a dynamic relaxation procedure, as presented in [35,36,38,39]. Material properties or axial stiffness of all members are also specified at the beginning [35,36,39]. Force density coefficients are considered as symbolic variables that cannot be applied for structures with large number of members [34]. Moreover, the obtained configurations cannot be ensured to be stable even though they are in self-equilibrium state [23].

The present paper is an extension of the authors' previous work [31] and is aimed at form-finding of free-form tensegrity structures in which both classes 1 and 2 of tensegrities are investigated. The topology and the initial force density vector, which is randomly generated with the sign of each component of this vector based on the types of members, are the required information in this form-finding process. The eigenvalue decomposition (EVD) of the force density matrix and the singular value decomposition (SVD) of the equilibrium matrix are performed iteratively to find the feasible sets of nodal coordinates and force densities which satisfy the minimum required rank deficiencies of the force density and equilibrium matrices, respectively. Any assumption about initial nodal coordinates or member lengths, material properties and the positive semi-definite condition of the force density matrix [29] is not necessary in the proposed form-finding procedure, which is considered as the advantage of the proposed method compared to the available ones. The self-equilibrium state of free-form tensegrities can be achieved in a few of remarkable iterations. An approach of defining a unique configuration of free-form tensegrity structures by specifying an independent set of nodal coordinates is rigorously provided, which implies that the geometrical and mechanical properties of the structure can be at least partly controlled by the proposed method.

2 Self-equilibrium equations and rank deficiency conditions

2.1 Basic assumptions

In this study, the following assumptions are made in tensegrity structures:

- The topology of the structure in terms of nodal connectivity is known.
- Members are connected by pin joints.
- No external load is applied and the self-weight of the structure is neglected during the form-finding procedure.
- There are no dissipative forces acting on the system.
- Both local and global buckling are not considered.

2.2 Self-equilibrium equations

For a d-dimensional ($d = 2$ or 3) tensegrity structure with b members, n free nodes and n_f fixed nodes (supports), its topology can be expressed by a connectivity matrix $\mathbf{C}_s(\in\mathbb{R}^{b\times(n+n_f)})$ as discussed in [31,40]. Suppose member k connects nodes i and j ($i < j$), then the ith and jth elements of the kth row of $\mathbf{C}_s$ are set to 1 and -1, respectively, as follows:

$$\mathbf{C}_{s(k,p)} = \begin{cases} 1 & \text{for } p = i, \\ -1 & \text{for } p = j, \\ 0 & \text{otherwise.} \end{cases} \tag{1}$$

If the free nodes are numbered first, then the fixed nodes, $\mathbf{C}_s$ can be divided into two parts as

$$\mathbf{C}_s = [\mathbf{C}\ \mathbf{C}_f] \tag{2}$$

where $\mathbf{C}(\in\mathbb{R}^{b\times n})$ and $\mathbf{C}_f(\in\mathbb{R}^{b\times n_f})$ describe the connectivities of the members to the free and fixed nodes, respectively. Let $\mathbf{x}$, $\mathbf{y}$, $\mathbf{z}(\in\mathbb{R}^n)$ and $\mathbf{x}_f$, $\mathbf{y}_f$, $\mathbf{z}_f(\in\mathbb{R}^{n_f})$ denote the nodal coordinate vectors of the free and fixed nodes, respectively, in x-, y- and z-directions.

The equilibrium equations of the free nodes in each direction of a general pin-jointed structure given by [24] can be stated as

$$\mathbf{C}^T\mathrm{diag}(\mathbf{q})\mathbf{C}\mathbf{x} + \mathbf{C}^T\mathrm{diag}(\mathbf{q})\mathbf{C}_f\mathbf{x}_f = \mathbf{p}_x, \tag{3.1}$$

$$\mathbf{C}^T\mathrm{diag}(\mathbf{q})\mathbf{C}\mathbf{y} + \mathbf{C}^T\mathrm{diag}(\mathbf{q})\mathbf{C}_f\mathbf{y}_f = \mathbf{p}_y, \tag{3.2}$$

$$\mathbf{C}^T\mathrm{diag}(\mathbf{q})\mathbf{C}\mathbf{z} + \mathbf{C}^T\mathrm{diag}(\mathbf{q})\mathbf{C}_f\mathbf{z}_f = \mathbf{p}_z \tag{3.3}$$

where $\mathbf{p}_x$, $\mathbf{p}_y$ and $\mathbf{p}_z$ ($\in\mathbb{R}^n$) are the vectors of external loads applied at the free nodes in x-, y- and z-directions, respectively. The symbol, $(\cdot)^T$, denotes the transpose of a matrix or vector. And $\mathrm{diag}(\mathbf{q})(\in\mathbb{R}^{b\times b})$ is a diagonal square matrix of $\mathbf{q}(\in\mathbb{R}^b)$ which is the force density vector as suggested in [24], defined by

$$\mathbf{q} = \{q_1, q_2, \ldots, q_b\}^T \tag{4}$$

in which each component of this vector is the force f_k to length l_k ratio $q_k = f_k/l_k (k = 1, 2, \ldots, b)$ known as force density or self-stressed coefficient in [23].

When external load and self-weight are ignored, the tensegrity system does not require any fixed nodes (supports). Its geometry can be defined by the relative position of the nodes. That is, the system can be considered as a free-standing rigid-body in space [31,40]. In this context, Eq. (3.1) becomes:

$$\mathbf{D}\mathbf{x} = \mathbf{0}, \tag{5.1}$$

$$\mathbf{D}\mathbf{y} = \mathbf{0}, \tag{5.2}$$

$$\mathbf{D}\mathbf{z} = \mathbf{0} \tag{5.3}$$

where $\mathbf{D}(\in\mathbb{R}^{n\times n})$ known as force density matrix [29,34] or stress matrix [20,41,42] is given by

$$\mathbf{D} = \mathbf{C}^T \text{diag}(\mathbf{q})\mathbf{C}. \tag{6}$$

For simplicity, Eq. (5.1) can be reorganized as

$$\mathbf{D}[\mathbf{x}\ \mathbf{y}\ \mathbf{z}] = [\mathbf{0}\ \mathbf{0}\ \mathbf{0}] \tag{7}$$

where $[\mathbf{x}\ \mathbf{y}\ \mathbf{z}](\in\mathbb{R}^{n\times d})$ is a matrix of nodal coordinates for a d-dimensional ($d = 2$ or 3) tensegrity structure.

On the other hand, by substituting Eq. (6) into (5.1), the self-equilibrium equations of the tensegrity structures can also be reorganized as

$$\mathbf{A}\mathbf{q} = \mathbf{0} \tag{8}$$

where $\mathbf{A}$ $(\in\mathbb{R}^{dn\times b})$ is known as the equilibrium matrix in [31,40], defined by

$$\mathbf{A} = \begin{pmatrix} \mathbf{C}^T \text{diag}(\mathbf{C}\mathbf{x}) \\ \mathbf{C}^T \text{diag}(\mathbf{C}\mathbf{y}) \\ \mathbf{C}^T \text{diag}(\mathbf{C}\mathbf{z}) \end{pmatrix}. \tag{9}$$

Equation (7) presents the relation between the force densities and the nodal coordinates, while Eq. (8) shows the relation between the projected lengths $\mathbf{C}\mathbf{x}$, $\mathbf{C}\mathbf{y}$, $\mathbf{C}\mathbf{z}$ in x-, y-, z-directions, respectively, and the force densities. Both Eqs. (7) and (8) are linear homogeneous systems of the self-equilibrium equations with respect to the nodal coordinates and the force densities, respectively.

2.3 Rank deficiency conditions

From Eq. (6), $\mathbf{D}$ is always square, symmetric and singular with a nullity of at least one since the sum of all components in any row or column is zero for any tensegrity structure [31,34]. Hence, the vector $\bar{\mathbf{I}}_1 = \{1, 1, \ldots, 1\}^T (\in \mathbb{R}^n)$ is a solution of Eq. (5.1). There are two rank deficiency conditions that need to be considered [31]. The first one related to the semi-definite matrix $\mathbf{D}$ of Eq. (7) is defined by

$$n_{\mathbf{D}} \geq d + 1 \tag{10}$$

where $n_{\mathbf{D}}(=n - r_{\mathbf{D}})$ denotes the dimension of the null space of $\mathbf{D}$ or rank deficiency of $\mathbf{D}$; and $r_{\mathbf{D}} = \text{rank}(\mathbf{D})$. This condition forces Eq. (7) to yield at least d useful particular solutions [45], which exclude the above vector $\bar{\mathbf{I}}_1$ due to degenerating geometry of the tensegrity structure [31,34]. These d particular solutions form a vector space basis for generating a d-dimensional tensegrity structure.

The second-rank deficiency condition related to matrix $\mathbf{A}$ of Eq. (8) which ensures the existence of at least one state of self-stress can be stated as

$$s = n_{\mathbf{A}} \geq 1 \tag{11}$$

where $n_{\mathbf{A}}(=b - r_{\mathbf{A}})$ denotes the dimension of the null space of $\mathbf{A}$ or rank deficiency of $\mathbf{A}$; $r_{\mathbf{A}} = \text{rank}(\mathbf{A})$; and s is known as the number of independent states of self-stress, while the number of inextensional mechanisms as presented in [43,44] is computed by

$$m = dn - r_{\mathbf{A}}. \tag{12}$$

Note that since the tensegrity structure is free-standing, it possesses two types of mechanisms: rigid-body mechanisms (rigid-body motions) and infinitesimal mechanisms. The number of infinitesimal mechanisms m_{in} is determined by excluding $r_b(=d(d+1)/2)$ independent rigid-body mechanisms in m inextensional mechanisms above.

3 Form-finding process

The initial force density vector is randomly generated as follows with the sign of each component of this vector based on the type of each member, i.e. either cable or strut which is under tension or compression, respectively:

$$\mathbf{q}^0 = \{\underbrace{+r_1 \ +r_2 \cdots +r_c}_{\text{cables}} \ \ \underbrace{-r_{c+1} \ -r_{c+2} \cdots -r_b}_{\text{struts}}\}^T \tag{13}$$

where $r_1, r_2, \ldots, r_c, r_{c+1}, r_{c+2}, \ldots, r_b$ are all random numbers distributed in the interval (0, 10); and c denotes the number of cables. Note to keep positive sign for cables (tension) and negative for struts (compression). While in the previous method [31], the components of this vector consist of unitary entries $+1$ and -1 for cables and struts, respectively.

Subsequently, the force density matrix $\mathbf{D}$ is calculated from $\mathbf{q}^0$ by Eq. (6). After that, the nodal coordinates are selected from the EVD of the matrix $\mathbf{D}$, which is discussed in Sect. 2.1. These nodal coordinates are substituted into Eq. (8) to define the force density vector $\mathbf{q}$ by the SVD of the equilibrium matrix $\mathbf{A}$, which is presented in Sect. 2.2. The force density matrix $\mathbf{D}$ is then updated by Eq. (6). The process is calculated iteratively for searching two feasible sets of nodal coordinates $[\mathbf{x}\ \mathbf{y}\ \mathbf{z}]$ and force densities $\mathbf{q}$ until the rank deficiencies of Eqs. (10) and (11) are satisfied, which forces Eqs. (7) and (8) to become true. In this context, at least one state of self-stress can be created, $s \geq 1$. In this study, based on required rank deficiencies from Eqs. (10) and (11), the form-finding process is stopped as

$$n^*_{\mathbf{D}} = d + 1, \tag{14.1}$$

$$n^*_{\mathbf{A}} = 1 \tag{14.2}$$

where $n^*_{\mathbf{D}}$ and $n^*_{\mathbf{A}}$ are minimum required rank deficiencies of the force density and equilibrium matrices, respectively.

3.1 Determination of a feasible set of nodal coordinates

The square symmetric force density matrix $\mathbf{D}$ can be factorized as follows by using the EVD [45]:

$$\mathbf{D} = \Phi \Lambda \Phi^T \tag{15}$$

where $\Phi (\in \mathbb{R}^{n \times n})$ is the orthogonal matrix ($\Phi\Phi^T = \mathbf{I}_n$, in which $\mathbf{I}_n \in \mathbb{R}^{n \times n}$ is the unit matrix) whose ith column is the eigenvector basis $\boldsymbol{\phi}_i (\in \mathbb{R}^n)$ of $\mathbf{D}$. $\Lambda (\in \mathbb{R}^{n \times n})$ is the diagonal matrix whose diagonal elements are the corresponding eigenvalues, i.e., $\Lambda_{ii} = \lambda_i$. The eigenvector $\boldsymbol{\phi}_i$ of Φ corresponds to eigenvalue λ_i of Λ. The eigenvalues are in increasing order $\lambda_1 \leq \lambda_2 \leq \cdots \leq \lambda_n$. It is clear that the number of zero eigenvalues of $\mathbf{D}$ is equal to the dimension of its null space. Let p be the number of zero and negative eigenvalues of $\mathbf{D}$. There are two cases that need to be considered. The first one is $p \leq n^*_{\mathbf{D}}$, and the other is $p > n^*_{\mathbf{D}}$.

Case 1 The first $n^*_{\mathbf{D}}$ orthonormal eigenvectors of Φ are directly taken as potential nodal coordinates

$$[\mathbf{x}\ \mathbf{y}\ \mathbf{z}] \in \bar{\Phi} = [\boldsymbol{\phi}_1\ \boldsymbol{\phi}_2 \cdots \boldsymbol{\phi}_{n^*_{\mathbf{D}}}]. \tag{16}$$

The force density vector $\mathbf{q}$, which is repeatedly approximated from Eq. (25), is in fact the least-square solution of the linear homogeneous system Eq. (8) solved by the SVD technique of the equilibrium matrix $\mathbf{A}$ as presented in Sect. 3.2. In other words, the algorithm iteratively modifies the force density vector $\mathbf{q}$ as small as possible to make the first $n^*_{\mathbf{D}}$ eigenvalues of $\mathbf{D}$ become null as

$$\lambda_i = 0, \quad (i = 1, 2, \ldots, n^*_{\mathbf{D}}). \tag{17}$$

All the projected lengths $\mathbf{L} (\in \mathbb{R}^{b \times n^*_{\mathbf{D}}})$ of $\bar{\Phi}$ along $n^*_{\mathbf{D}}$ directions for b members are computed by

$$\mathbf{L} = \mathbf{C}\bar{\Phi} = \left[(\mathbf{C}\boldsymbol{\phi}_1)\ (\mathbf{C}\boldsymbol{\phi}_2) \cdots \left(\mathbf{C}\boldsymbol{\phi}_{n^*_{\mathbf{D}}}\right) \right] \tag{18}$$

to remove one vector $\boldsymbol{\phi}_i$ among $n^*_{\mathbf{D}}$ eigenvector bases of $\bar{\Phi}$ if

$$\mathbf{C}\boldsymbol{\phi}_i = \mathbf{0} \tag{19}$$

or which $\boldsymbol{\phi}_i$ causes a zero length to any member among b members of the structure whose lengths are defined by

$$l_k = \sqrt{\left(l_k^x\right)^2 + \left(l_k^y\right)^2 + \left(l_k^z\right)^2} \tag{20}$$

where $l_k(=\mathbf{l}) \in \mathbb{R}^b$ ($k = 1, 2, \ldots, b$; and assuming $d = 3$) indicates the vector of lengths of b members from any combination of d singular vectors among $n_{\mathbf{D}}^*$ above singular vector bases in d-dimensional space; and $l_k^x(=\mathbf{l}^x)$, $l_k^y(=\mathbf{l}^y)$ and $l_k^z(=\mathbf{l}^z) \in \mathbb{R}^b$ denote the coordinate difference vectors of the b members in x-, y- and z-directions, respectively, which are calculated from

$$\begin{aligned} \mathbf{l}^x &= \mathbf{C}\boldsymbol{\phi}_i, \\ \mathbf{l}^y &= \mathbf{C}\boldsymbol{\phi}_j \quad (\boldsymbol{\phi}_i, \boldsymbol{\phi}_j, \boldsymbol{\phi}_k \in \bar{\Phi}), \\ \mathbf{l}^z &= \mathbf{C}\boldsymbol{\phi}_k. \end{aligned} \tag{21}$$

Equation (19) shows that $\boldsymbol{\phi}_i$ is linearly dependent with the above vector $\bar{\mathbf{I}}_1$, while Eq. (20) is very useful in checking whether there exists any member with zero length (a zero length of a member exists when its two nodes coincide with each other) among b members of a d-dimensional structure. If there is no $\boldsymbol{\phi}_i$ that satisfies Eq. (19) or causes a zero length to any member of the structure, the first three eigenvectors of $\bar{\Phi}$ are chosen as nodal coordinates [**x y z**] for the three-dimensional tensegrity structure.

Accordingly, **D** will finally have the required rank deficiency $n_{\mathbf{D}}^*$ without any negative eigenvalue. It implies that **D** is positive semi-definite, and any tensegrity structure falling into this case is super stable regardless of material properties and level of self-stress coefficients [42,46].

Case 2 Where $p > n_{\mathbf{D}}^*$, the rank deficiency may be forced to be larger than required or sufficient, but **D** may not be positive semi-definite during iteration. Additionally, the proposed form-finding procedure will evaluate the tangent stiffness matrix of the tensegrity structure, which is given in [28,47–49]. If the tangent stiffness matrix is positive-definite, then the structure is stable when its rigid-body motions are constrained. Using this criterion, the stability of any pre-stressed or tensegrity structure can be controlled by checking the eigenvalues of its tangent stiffness matrix (for more details, see [31]).

In short, the best scenario of configuration in three-dimensional space is formed by the three best candidate eigenvectors selected from the first four eigenvector bases which correspond to the first four smallest eigenvalues, respectively. These eigenvalues will be gradually modified to be zero by the proposed iterative form-finding algorithm. In other words, the proposed form-finding procedure has repeatedly approximated the equilibrium configuration such that

$$\mathbf{D}[\mathbf{x}\ \mathbf{y}\ \mathbf{z}] \approx [\mathbf{0}\ \mathbf{0}\ \mathbf{0}]. \tag{22}$$

3.2 Determination of the feasible set of force densities

The equilibrium matrix **A** is computed by substituting the set of approximated nodal coordinates [**x y z**] from Eq. (22) into (9). In order to solve the linear homogeneous system Eq. (8), the SVD [45] is carried out on the equilibrium matrix **A**:

$$\mathbf{A} = \mathbf{U}\mathbf{V}\mathbf{W}^T \tag{23}$$

where $\mathbf{U}(\in\mathbb{R}^{dn\times dn}) = [\mathbf{u}_1\mathbf{u}_2\cdots\mathbf{u}_{dn}]$ and $\mathbf{W}(\in\mathbb{R}^{b\times b}) = [\mathbf{w}_1\mathbf{w}_2\cdots\mathbf{w}_b]$ are orthogonal matrices. $\mathbf{V}(\in\mathbb{R}^{dn\times b})$ is a diagonal matrix with non-negative singular values of **A** in decreasing order as

$$\sigma_1 \geq \sigma_2 \geq \cdots \geq \sigma_b \geq 0. \tag{24}$$

As indicated in Eq. (14.2), the iterative form-finding algorithm is successful in case of $n_{\mathbf{A}}^* = 1$. Accordingly, there are also two cases for s during the iterative form-finding procedure:

Case 1 $s = 0$, there exists no null space of **A**. The form-finding procedure defines the approximated **q** that matches in signs with $\mathbf{q}^0$, as presented in [31], such that

$$\mathbf{A}\mathbf{q} \approx \mathbf{0}. \tag{25}$$

Case 2 $s = 1$, it is known [50] that the bases of vector spaces of force densities and mechanisms of any tensegrity structure are calculated from the null spaces of the equilibrium matrix. In this case, the matrices $\mathbf{U}$ and $\mathbf{W}$ from Eq. (23) can be expressed, respectively, as

$$\mathbf{U} = [\mathbf{u}_1 \mathbf{u}_2 \cdots \mathbf{u}_{r_\mathbf{A}} | \mathbf{m}_1 \cdots \mathbf{m}_m], \tag{26.1}$$

$$\mathbf{W} = [\mathbf{w}_1 \mathbf{w}_2 \cdots \mathbf{w}_{b-1} | \mathbf{q}_1] \tag{26.2}$$

where the vectors $\mathbf{m}_i \in \mathbb{R}^{dn} (i = 1, 2, \ldots, m)$ denote the m inextensional mechanisms; and the vector $\mathbf{q}_1 (\in \mathbb{R}^b)$ matching in signs with $\mathbf{q}^0$ is indeed the single state of self-stress which satisfies the homogeneous Eq. (8).

In summary, the EVD of the force density matrix $\mathbf{D}$ and the SVD of the equilibrium matrix $\mathbf{A}$ are performed iteratively to find the feasible sets of nodal coordinates $[\mathbf{x}\ \mathbf{y}\ \mathbf{z}]$ and force density vector $\mathbf{q}$ by selecting the appropriate singular vector bases in each decomposition as the least-square solutions until the minimum required rank deficiencies of these two matrices are satisfied, respectively, as presented in Eq. (14.1).

Since the tensegrity structure should satisfy the self-equilibrium conditions, the vectors of unbalanced internal forces ε_x, ε_y and $\varepsilon_z (\in \mathbb{R}^n)$ in x-, y- and z-directions, respectively, defined as follows can be employed for evaluating the accuracy of the results:

$$\varepsilon_x = \mathbf{D}\mathbf{x}, \tag{27.1}$$

$$\varepsilon_y = \mathbf{D}\mathbf{y}, \tag{27.2}$$

$$\varepsilon_z = \mathbf{D}\mathbf{z}. \tag{27.3}$$

The Euclidean norm is utilized to define the design error ϵ as

$$\epsilon = \sqrt{(\varepsilon_x)^T \varepsilon_x + (\varepsilon_y)^T \varepsilon_y + (\varepsilon_z)^T \varepsilon_z}. \tag{28}$$

3.3 Determination of the unique configuration

A new approach of defining the unique configuration of free-form tensegrity structures is fully described in this Section. Once the feasible sets of nodal coordinates and force densities are obtained, the unique configuration of free-form tensegrities can be defined by specifying the independent set of nodal coordinates. It is noted that from Eqs. (7) and (14.1) there are $(n^*_\mathbf{D} \times d)$ components of $n^*_\mathbf{D}$ independent nodes [23] in the matrix of nodal coordinates $[\mathbf{x}\ \mathbf{y}\ \mathbf{z}]$ that can be arbitrarily specified, because the value of the rank deficiency of matrix $\mathbf{D}$ is $n^*_\mathbf{D}$. The solution of Eq. (7) can be stated as

$$[\mathbf{x}\ \mathbf{y}\ \mathbf{z}] = \mathbf{N}\mathbf{B} \tag{29}$$

where $\mathbf{B} (\in \mathbb{R}^{n^*_\mathbf{D} \times d})$ is the coefficient matrix obtained by specifying a matrix $[\bar{\mathbf{x}}\ \bar{\mathbf{y}}\ \bar{\mathbf{z}}] (\in \mathbb{R}^{n^*_\mathbf{D} \times d})$ that consists of the given coordinates of a set of $n^*_\mathbf{D}$ independent nodes; $\mathbf{N} (\in \mathbb{R}^{n \times n^*_\mathbf{D}})$ is the null space of the $n^*_\mathbf{D}$ rank deficient matrix $\mathbf{D}$, which satisfies

$$\mathbf{D}\mathbf{N} = [\mathbf{0} \cdots \mathbf{0}]_{(n \times n^*_\mathbf{D})}. \tag{30}$$

Let $\Gamma \subset \{1, 2, \ldots, n\}$ denote the set of indices of the $n^*_\mathbf{D}$ independent nodes whose coordinates are to be specified among n nodes of the structure. $[\bar{\mathbf{x}}\ \bar{\mathbf{y}}\ \bar{\mathbf{z}}]$ is defined as the given nodal coordinates matrix consisting of coordinates $[x_j\ y_j\ z_j] (j \in \Gamma)$ of the above $n^*_\mathbf{D}$ independent nodes that are specified by designers. By assembling the corresponding rows of $\mathbf{N}$ based on Γ to generate a submatrix $\bar{\mathbf{N}} (\in \mathbb{R}^{n^*_\mathbf{D} \times n^*_\mathbf{D}})$, the relation between $[\bar{\mathbf{x}}\ \bar{\mathbf{y}}\ \bar{\mathbf{z}}]$ and $\mathbf{B}$ can be expressed as

$$[\bar{\mathbf{x}}\ \bar{\mathbf{y}}\ \bar{\mathbf{z}}] = \bar{\mathbf{N}}\mathbf{B}. \tag{31}$$

If $\bar{\mathbf{N}}$ is full-rank, i.e. $\text{rank}(\bar{\mathbf{N}}) = n^*_\mathbf{D}$, Eq. (31) can be solved as

$$\mathbf{B} = \bar{\mathbf{N}}^{-1} [\bar{\mathbf{x}}\ \bar{\mathbf{y}}\ \bar{\mathbf{z}}]. \tag{32}$$

By substituting $\mathbf{B}$ into Eq. (29), the matrix of coordinates $[\mathbf{x}\ \mathbf{y}\ \mathbf{z}]$ of all nodes is obtained as

$$[\mathbf{x}\ \mathbf{y}\ \mathbf{z}] = \mathbf{N}\bar{\mathbf{N}}^{-1} [\bar{\mathbf{x}}\ \bar{\mathbf{y}}\ \bar{\mathbf{z}}]. \tag{33}$$

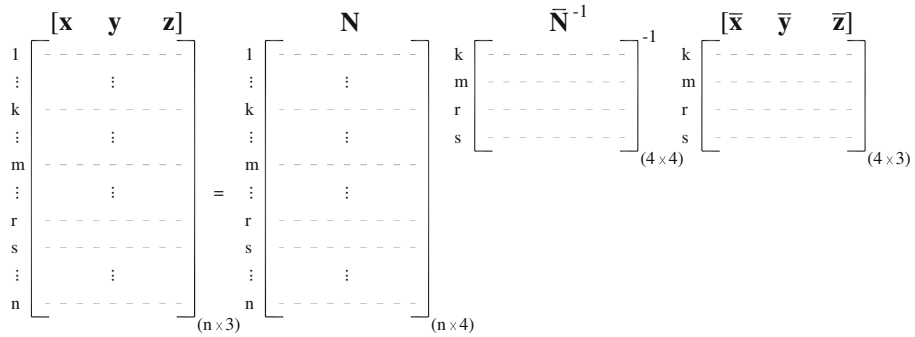

Fig. 2 Graphical illustration of defining the unique configuration of the three-dimensional tensegrity structure in terms of nodal coordinates. Note that k, m, r and s are the four arbitrarily independent nodes corresponding to kth, mth, rth and sth row of matrix $\mathbf{N}$, whose nodal coordinates can be specified to define a unique solution of coordinates of n nodes

Note that the rank of $[\bar{\mathbf{x}}\ \bar{\mathbf{y}}\ \bar{\mathbf{z}}]$ must be equal to d to avoid obtaining degenerate d-dimensional tensegrity structures. Equation (33) can be expressed explicitly by Fig. 2. Let N_j denote the jth row vector of $\mathbf{N}$ corresponding to the node number j. The following algorithm generates Γ and $\bar{\mathbf{N}}$.

Algorithm 1

- *Step 0*: Let $\Gamma = \emptyset$, $\hat{\mathbf{N}} = \emptyset$, and feasible set $\Psi = \{1, 2, \ldots, n\}$. Set $i = 0$.
- *Step 1*: If $i = n^*_{\mathbf{D}}$, then $\bar{\mathbf{N}} = \hat{\mathbf{N}}$, and STOP. Otherwise, set $i = i + 1$.
- *Step 2*: Choose node number $j(\in \Psi)$ whose coordinates are to be specified. Add this node to the set of indices of the independent nodes $\Gamma = \Gamma \cup j$, and simultaneously remove it from the feasible set $\Psi = \Psi \backslash j$.
- *Step 3*: Determine $\mathbf{N}$ by Eq. (30). Choose N_j, then generate $\hat{\mathbf{N}}$ by adding N_j to matrix $\hat{\mathbf{N}}$, i.e., $\hat{\mathbf{N}} = \hat{\mathbf{N}} \cup N_j$, and go to *Step 1*.

3.4 Form-finding procedure for free-form tensegrity structures

Two sets of parameters that are the nodal coordinates and the force density vector of the free-form tensegrity structures can be simultaneously defined by the proposed form-finding through the following procedure. An approach of defining the unique configuration of tensegrities based on a specified independent set of nodal coordinates is also provided.

Form-finding procedure

- *Step 1*: Define $\mathbf{C}$ by Eq. (1) for the given topology of the tensegrity structure.
- *Step 2*: Specify the types of members to randomly generate the initial force density vector $\mathbf{q}^0$ by Eq. (13). Set $i = 0$.
- *Step 3*: Calculate $\mathbf{D}^i$ using Eq. (6).
- *Step 4*: Carry out Eq. (15) to define $[\mathbf{x}\ \mathbf{y}\ \mathbf{z}]^i$ through Eq. (22).
- *Step 5*: Determine $\mathbf{A}^i$ by Eq. (9).
- *Step 6*: Perform Eq. (23) to define $\mathbf{q}^{i+1}$ through Eq. (25).
- *Step 7*: Define $\mathbf{D}^{i+1}$ with $\mathbf{q}^{i+1}$ by Eq. (6). If Eq. (14.1) is satisfied, the solutions exist. Otherwise, set $i = i + 1$ and return to *Step 4*.
- *Step 8*: The process is terminated until Eq. (28) has been checked. The final coordinates and force density vector are the solutions. Otherwise, set $i = i + 1$ and return to *Step 4*.
- *Step 9*: If you want to obtain the unique configuration, then specify $[\bar{\mathbf{x}}\ \bar{\mathbf{y}}\ \bar{\mathbf{z}}]$ and define $\bar{\mathbf{N}}$ by using Algorithm 1. Otherwise, STOP.
- *Step 10*: Define the unique configuration in terms of $[\mathbf{x}\ \mathbf{y}\ \mathbf{z}]$ by Eq. (33).

4 Numerical examples

Numerical examples are presented for several free-form tensegrity structures using Matlab Version 7.4 (R2007a) [51]. Based on the algorithm developed, both the *nodal coordinates* and the *force density vector* are

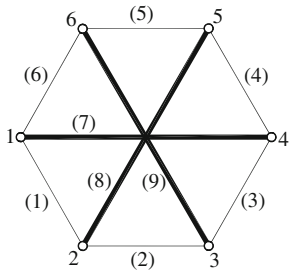

Fig. 3 A two-dimensional hexagonal tensegrity structure. The *thick and thin lines* represent the struts and cables, respectively

Table 1 The force density coefficients and lengths of the 2-D regular and free-form hexagonal tensegrity structure

Elements	Initial value		Final value			
	$\mathbf{q}^0$		$\mathbf{q}$		$\mathbf{l}$	
	Regular (Ref. [31])	Free-form (Present)	Regular (Ref. [31])	Free-form (Present)	Regular (Ref. [31])	Free-form (Present)
1	1	5.4701	1.0	1.0000	0.5774	1.5000
2	1	2.9632	1.0	0.3359	0.5774	1.8185
3	1	7.4469	1.0	1.0316	0.5774	1.6262
4	1	1.8896	1.0	0.6063	0.5774	2.7581
5	1	6.8678	1.0	0.6775	0.5774	1.1442
6	1	1.8351	1.0	0.4915	0.5774	3.1245
7	−1	−3.6848	−0.5	−0.1645	1.1547	2.0000
8	−1	−6.2562	−0.5	−0.3439	1.1547	4.6036
9	−1	−7.8023	−0.5	−0.3654	1.1547	4.8062

simultaneously defined with limited information of the nodal connectivity and the initial randomly generated force density vector. The *unique configuration* of the tensegrity structure can also be defined by specifying the independent set of nodal coordinates. A hexagon, expandable octahedron, truncated icosahedron and seven-strut cylindrical tensegrities belong to class 1, while the octahedral cell tensegrity is of class 2.

4.1 Two-dimensional free-form tensegrity structures

4.1.1 Hexagon

The initial topology of the hexagonal tensegrity structure comprising three struts and six cables (Fig. 3) was studied by Tran and Lee [31] for its regular form. The known information is the incidence matrix $\mathbf{C}$ and the initial force density vector $\mathbf{q}^0$, which is randomly generated by the proposed form-finding procedure as listed in Table 1. The obtained force density vector $\mathbf{q}$ normalized with respect to the force density coefficient of the cable 1 is presented in Table 1.

Once the EVD of the force density matrix $\mathbf{D}$ and the SVD of the equilibrium matrix $\mathbf{A}$ are calculated, the values of their rank deficiencies are easily determined by counting the number of zero eigenvalues and zero singular values, respectively. A threshold value Tol($=10^{-10}$) is set in this study. All eigenvalues and singular values smaller than Tol are considered as zero, and the rank deficiencies as well as the ranks of $\mathbf{D}$ and $\mathbf{A}$ are defined accordingly. In this example, at the third iteration the obtained eigenvalues of matrix $\mathbf{D}$ are as follows:

$$0 \approx \lambda_1 < \lambda_2 < \lambda_3 = 3.1900 \times 10^{-13} < \text{Tol} < \lambda_4 = 1.7877 < \cdots < \lambda_6 = 2.4716 \tag{34}$$

which means $n_{\mathbf{D}} = 3$; i.e., $r_{\mathbf{D}} = n - n_{\mathbf{D}} = 6 - 3 = 3$. Hence, $\mathbf{D}$ satisfies the minimum required rank deficiency condition as mentioned in Eq. (14.1). While the obtained singular values of matrix $\mathbf{A}$ are

$$\sigma_1 = 1.8919 > \sigma_2 > \cdots > \sigma_8 = 0.4072 > \text{Tol} > \sigma_9 = 7.6090 \times 10^{-12} \approx 0 \tag{35}$$

which also means $n_{\mathbf{A}} = 1$; i.e., $r_{\mathbf{A}} = b - n_{\mathbf{A}} = 9 - 1 = 8$. Hence, $\mathbf{A}$ also satisfies the minimum required rank deficiency condition (Eq. (14.2)).

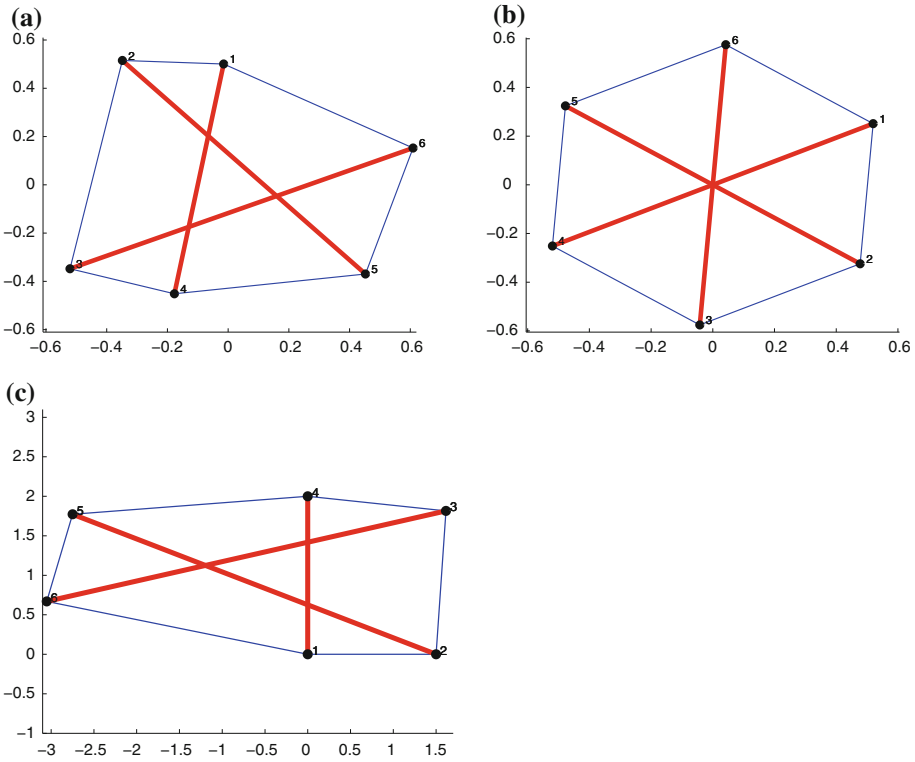

Fig. 4 The obtained geometry of the two-dimensional hexagonal tensegrity structure, **a** free-form shape, **b** regular shape (Ref. [31]), **c** free-form shape with the specified coordinates of a set of independent nodes

Table 2 The specified independent set of nodal coordinates of the 2-D free-form hexagonal tensegrity structure

Node	1	2	4
(x, y)	(0, 0)	(1.5, 0)	(0, 2)

The associated stable free-form configuration of the structure whose members' lengths are different from one another (as can be seen from Table 1) is plotted in Fig. 4a. It is thoroughly different from its regular form (Fig. 4b) presented by Ref. [31]. The form-finding procedure converges in three iterations with the design error $\epsilon = 2.033 \times 10^{-11}$. The structure obtained has only one self-stress state ($s = 1$) and one infinitesimal mechanism ($m = 1$) when its three rigid-body motions are constrained indicating it is statically and kinematically indeterminate [44].

If the coordinates of nodes 1, 2 and 4 are specified as shown in Table 2, the unique configuration of the structure can then be achieved by Eq. (33) and plotted in Fig. 4c. All members of the structure have different lengths compared to only one strut and one cable length of its regular counterpart in Fig. 4b. Therefore, by specifying the coordinates of the $n_{\mathbf{D}}^{*}(=3)$ independent nodes, the location of some members (e.g. members 1 and 7, which connect nodes 1 and 2, and nodes 1 and 4, respectively) as well as their lengths in the structure can be easily controlled.

4.2 Three-dimensional free-form tensegrity structures

4.2.1 Expandable octahedron

An expandable octahedron consisting of 6 struts and 24 cables (Fig. 5) was investigated first by Tibert and Pellegrino [34], Estrada et al. [29] and then by Tran and Lee [31] for its symmetric form. The initial randomly generated force density vector $\mathbf{q}^0$ and the calculated force density vector $\mathbf{q}$ after normalizing with respect to the force density coefficient of the cable 1 are reported in Table 3.

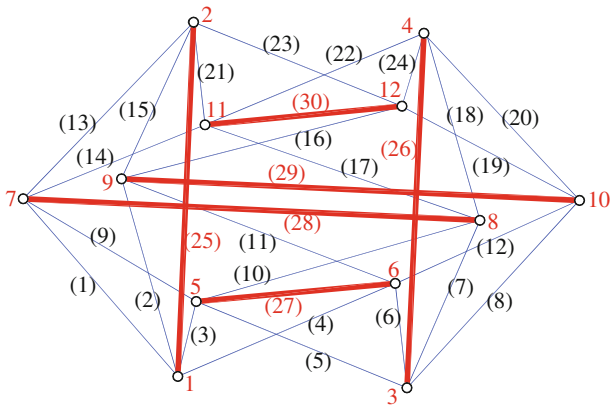

Fig. 5 An expandable octahedron tensegrity structure

Table 3 The force density coefficients and lengths of the regular and free-form expandable octahedron tensegrity structure

Elements	Initial value		Final value			
	$\mathbf{q}^0$		$\mathbf{q}$		$\mathbf{l}$	
	Regular (Ref. [31])	Free-form (Present)	Regular (Ref. [31])	Free-form (Present)	Regular (Ref. [31])	Free-form (Present)
1	1	3.8577	1.0	1.0000	0.5477	0.6683
2	1	6.8832	1.0	1.8755	0.5477	0.4038
3	1	9.6124	1.0	2.0442	0.5477	0.2732
4	1	9.4216	1.0	3.7029	0.5477	0.2998
5	1	5.1210	1.0	0.2334	0.5477	0.0933
6	1	3.1643	1.0	0.5660	0.5477	0.5733
7	1	7.8751	1.0	2.4219	0.5477	0.2325
8	1	7.8339	1.0	1.9283	0.5477	0.5851
9	1	7.6658	1.0	1.9903	0.5477	0.3503
10	1	7.6932	1.0	1.9688	0.5477	0.5559
11	1	1.9533	1.0	0.5696	0.5477	0.6983
12	1	7.1340	1.0	1.1547	0.5477	0.6854
13	1	5.1693	1.0	1.3680	0.5477	0.6749
14	1	2.9095	1.0	0.4481	0.5477	1.0443
15	1	1.8867	1.0	0.4962	0.5477	0.7762
16	1	8.4122	1.0	2.2148	0.5477	0.4704
17	1	2.5751	1.0	0.9185	0.5477	0.6693
18	1	2.4721	1.0	1.3417	0.5477	0.6493
19	1	6.9939	1.0	2.6782	0.5477	0.3022
20	1	9.0495	1.0	1.1022	0.5477	0.8439
21	1	5.6490	1.0	0.3302	0.5477	0.9613
22	1	7.3243	1.0	1.4515	0.5477	0.3155
23	1	2.3823	1.0	0.2819	0.5477	0.5491
24	1	9.5811	1.0	2.2933	0.5477	0.4397
25	−1	−5.8680	−1.5	−1.7221	0.8944	0.7389
26	−1	−7.1176	−1.5	−2.4570	0.8944	0.6798
27	−1	−1.3291	−1.5	−1.2125	0.8944	0.2460
28	−1	−8.2828	−1.5	−1.9214	0.8944	1.0403
29	−1	−7.7376	−1.5	−1.7577	0.8944	1.0384
30	−1	−2.0817	−1.5	−1.6561	0.8944	1.2654

The obtained stable free-form configuration of the structure is presented in Fig. 6. All members of the structure have different lengths, which makes it distinguished from its regular counterpart (Fig. 7) given by Ref. [31]. The form-finding procedure converges in eighteen iterations in comparison with thirteen iterations [31] for its regular form. The design error convergence is described in Fig. 8 with $\epsilon = 1.964 \times 10^{-9}$. The structure obtained has only one self-stress state ($s = 1$) and one infinitesimal mechanism ($m = 1$) except for its six rigid-body motions. Accordingly, it belongs to a statically and kinematically indeterminate structure [44].

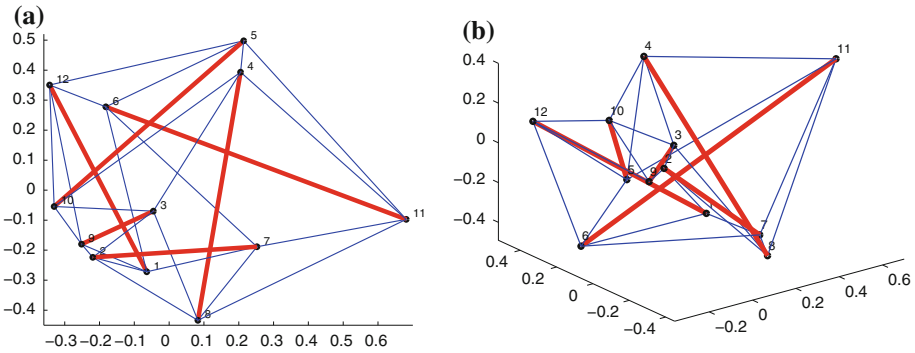

Fig. 6 The obtained free-form geometry of the expandable octahedron tensegrity structure, **a** top view, **b** perspective view

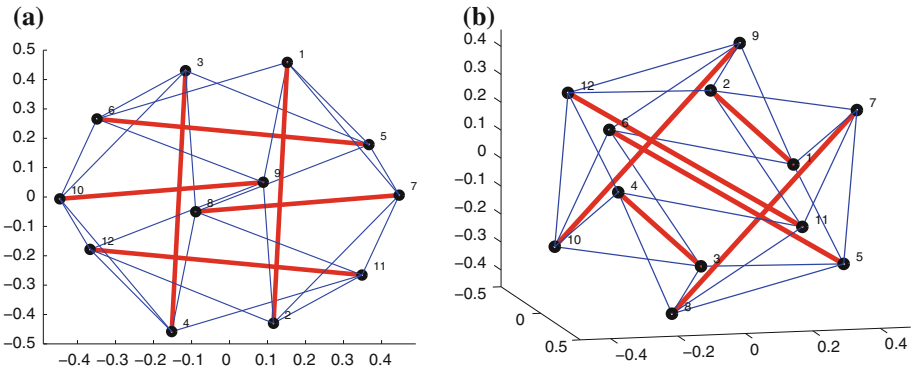

Fig. 7 The regular geometry of the expandable octahedron tensegrity structure (Ref. [31]), **a** top view, **b** perspective view

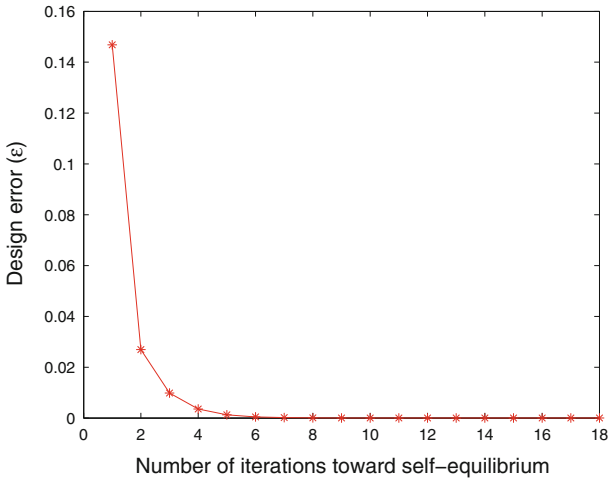

Fig. 8 The convergence of the proposed iterative algorithm for the free-form expandable octahedron

4.2.2 Truncated icosahedron

A more complicated example is the truncated icosahedron tensegrity system with 30 struts and 90 cables, which was analyzed by Estrada et al. [29] and then by Tran and Lee [31] for its regular form. The initial randomly generated force density vector $\mathbf{q}^0$ and the calculated force density vector $\mathbf{q}$ after normalizing with respect to the force density coefficient of the cable 1 are reported in Table 4. The obtained stable free-form configuration of the structure is plotted in Fig. 9. The design error ($\epsilon = 9.951 \times 10^{-9}$) is shown in Fig. 10 that exposes the convergence of the proposed form-finding in 66 iterations compared with 45 iterations [31] for its regular

Table 4 The initial random and obtained force density coefficients of the free-form truncated icosahedron tensegrity structure

$\mathbf{q}^0$	q_1^0	q_2^0	q_3^0	q_4^0	q_5^0	q_6^0	$\cdots$	q_{115}^0	q_{116}^0	q_{117}^0	q_{118}^0	q_{119}^0	q_{120}^0
	1.3902	1.2183	1.2183	1.0246	1.0248	1.0456	$\cdots$	−1.1168	−1.2282	−1.1923	−1.2693	−1.4959	−1.3776
$\mathbf{q}$	q_1	q_2	q_3	q_4	q_5	q_6	$\cdots$	q_{115}	q_{116}	q_{117}	q_{118}	q_{119}	q_{120}
	1.0000	2.0608	1.2391	1.3458	1.0040	2.2232	$\cdots$	−0.3387	−0.4622	−0.4094	−0.5970	−0.5007	−0.3750

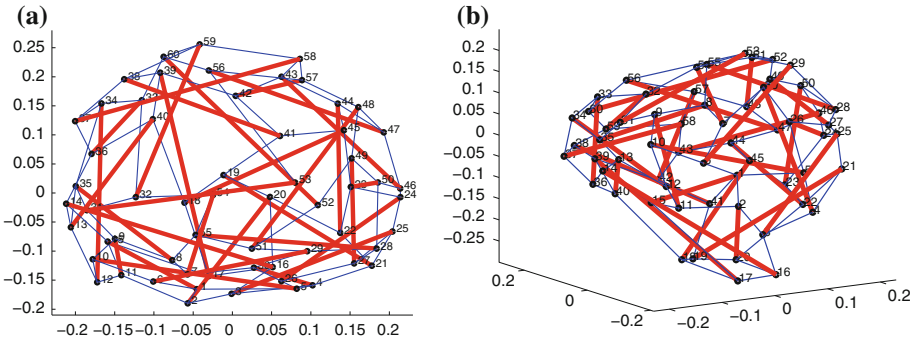

Fig. 9 The obtained free-form geometry of the truncated icosahedron tensegrity structure, **a** top view, **b** perspective view

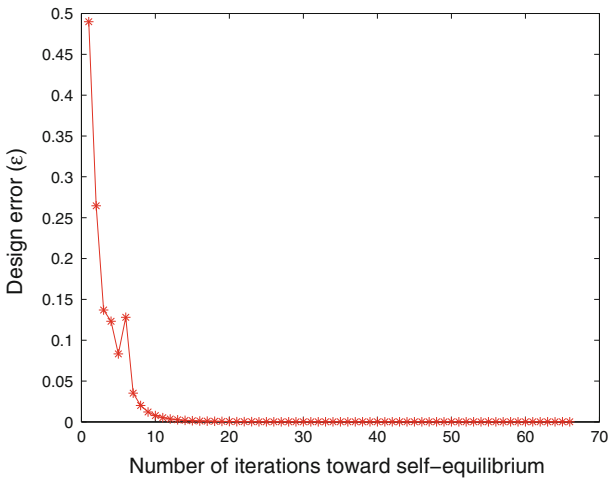

Fig. 10 The convergence of the proposed iterative algorithm for the free-form truncated icosahedron

form. It needs more iterations than the corresponding regular one. The obtained structure possesses one state of self-stress ($s = 1$) and 55 infinitesimal mechanisms ($m = 55$) excluding its six rigid-body motions.

4.2.3 Octahedral cell

The system shown in Fig. 11 has five struts and eight cables. Table 5 shows the initial randomly generated force density vector $\mathbf{q}^0$ and the calculated force density vector $\mathbf{q}$ after normalizing with respect to the force density coefficient of the cable 1. The achieved free-form configuration of the structure is displayed in Fig. 12. The form-finding procedure converges in four iterations with the design error $\epsilon = 1.000 \times 10^{-15}$. The structure obtained has only one state of self-stress ($s = 1$) and no infinitesimal mechanism ($m = 0$) after constraining its six rigid-body motions, indicating it is statically indeterminate and kinematically determinate [44]. If the coordinates of nodes 1, 2, 5 and 6 are specified as shown in Table 6, the unique free-form configuration of the structure can then be obtained and shown in Fig. 13.

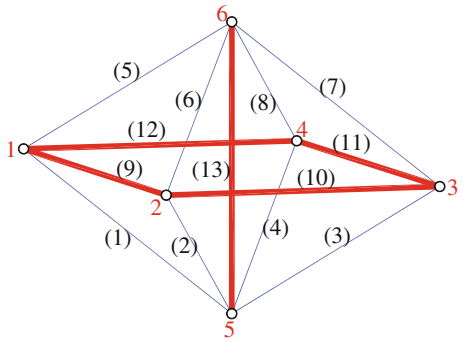

Fig. 11 An octahedral cell tensegrity structure

Table 5 The initial random and obtained force density coefficients of the free-form octahedral cell tensegrity structure

$\mathbf{q}^0$	q_1^0	q_2^0	q_3^0	q_4^0	q_5^0	q_6^0	q_7^0	q_8^0	q_9^0	q_{10}^0	q_{11}^0	q_{12}^0	q_{13}^0
	7.4313	3.9223	6.5548	1.7119	7.0605	0.3183	2.7692	0.4617	−0.9713	−8.2346	−6.9483	−3.1710	−9.5022
$\mathbf{q}$	q_1	q_2	q_3	q_4	q_5	q_6	q_7	q_8	q_9	q_{10}	q_{11}	q_{12}	q_{13}
	1.0000	0.5965	0.4306	0.8180	1.4545	0.7941	0.6567	1.1065	−0.8677	−0.6320	−0.7158	−1.0581	−1.6656

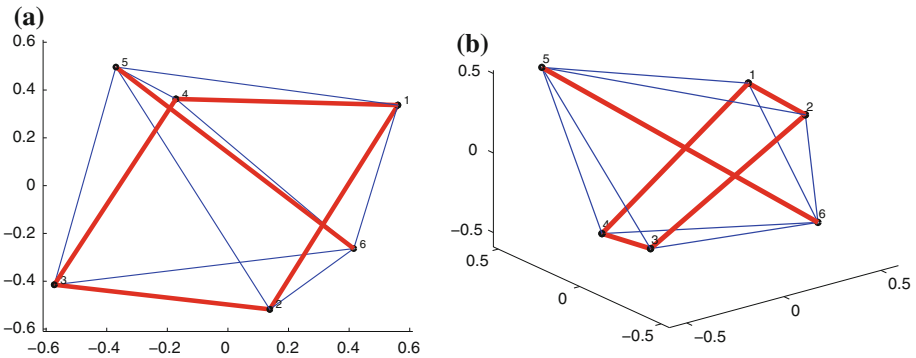

Fig. 12 The obtained free-form geometry of the octahedral cell tensegrity structure, **a** top view, **b** perspective view

Table 6 The specified independent set of nodal coordinates of the free-form octahedral cell tensegrity structure

Node	1	2	5	6
(x, y, z)	(−1, −1, 0)	(−1, 1, 0)	(0, 0, −1)	(0, 0, 1)

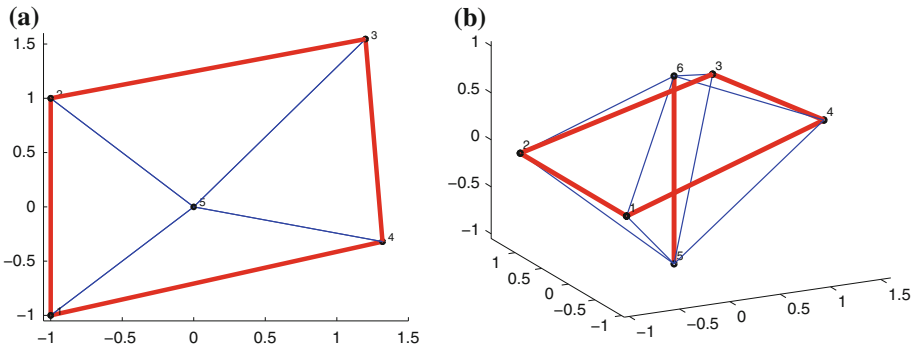

Fig. 13 The obtained free-form geometry of the octahedral cell tensegrity structure with the specified coordinates of a set of independent nodes, **a** top view, **b** perspective view

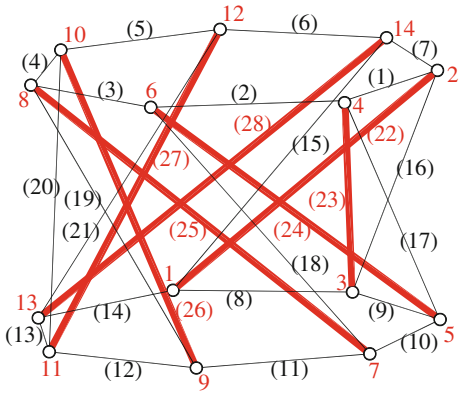

Fig. 14 A three-dimensional seven-strut cylindrical tensegrity structure

Table 7 The initial random and obtained force density coefficients of the seven-strut cylindrical tensegrity structure

$\mathbf{q}^0$	q_1^0	q_2^0	q_3^0	q_4^0	q_5^0	q_6^0	q_7^0	q_8^0	q_9^0	q_{10}^0	q_{11}^0	q_{12}^0	q_{13}^0	q_{14}^0
	9.2547	3.5726	7.8148	7.7836	4.4240	6.1104	1.6827	1.4856	5.7772	8.0125	9.4061	2.1692	6.1194	5.2245
	q_{15}^0	q_{16}^0	q_{17}^0	q_{18}^0	q_{19}^0	q_{20}^0	q_{21}^0	q_{22}^0	q_{23}^0	q_{24}^0	q_{25}^0	q_{26}^0	q_{27}^0	q_{28}^0
	1.1071	4.0341	2.4596	8.1486	3.8009	5.7568	2.4908	−6.4178	−3.3667	−6.8867	−7.2029	−7.7334	−5.0549	−1.7544
$\mathbf{q}$	q_1	q_2	q_3	q_4	q_5	q_6	q_7	q_8	q_9	q_{10}	q_{11}	q_{12}	q_{13}	q_{14}
	1.0000	0.6150	0.7928	0.6523	0.6779	2.1392	0.4703	0.3988	1.6935	0.9314	0.8808	0.6112	0.9084	0.4639
	q_{15}	q_{16}	q_{17}	q_{18}	q_{19}	q_{20}	q_{21}	q_{22}	q_{23}	q_{24}	q_{25}	q_{26}	q_{27}	q_{28}
	0.2956	0.4803	0.2912	0.9942	0.4569	1.0719	0.4569	−0.5328	−0.0839	−0.8039	−0.5116	−0.7162	−0.8003	−0.1693

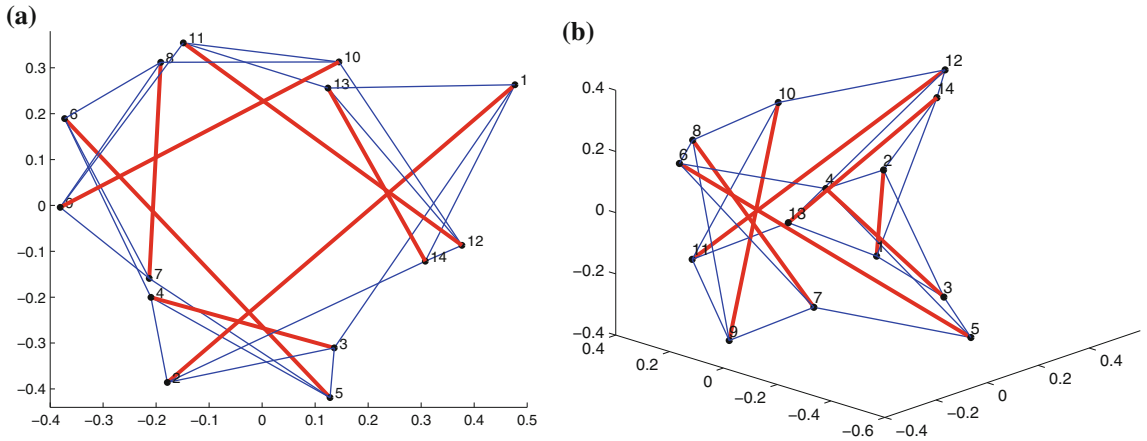

Fig. 15 The obtained free-form geometry of the seven-strut cylindrical tensegrity structure, **a** top view, **b** perspective view

4.2.4 Seven-strut cylindrical tensegrity

A three-dimensional seven-strut cylindrical tensegrity displayed in Fig. 14 has 7 struts and 21 cables. The initial randomly generated force density vector $\mathbf{q}^0$ and the calculated force density vector $\mathbf{q}$ after normalizing with respect to the force density coefficient of the cable 1 are displayed in Table 7. Figure 15 shows the obtained self-equilibrium stable free-form configuration. The design error convergence is described in Fig. 16 with $\epsilon = 1.964 \times 10^{-9}$ achieved within 32 iterations. The structure obtained has only one state of self-stress ($s = 1$) and nine infinitesimal mechanisms ($m = 9$) after constraining its six rigid-body motions, indicating it is statically and kinematically indeterminate [44]. Similarly, if the coordinates of $n_{\mathbf{D}}^*$ (=4) independent nodes 1, 2, 3 and 14 are specified as shown in Table 8, the unique free-form configuration of the structure can be

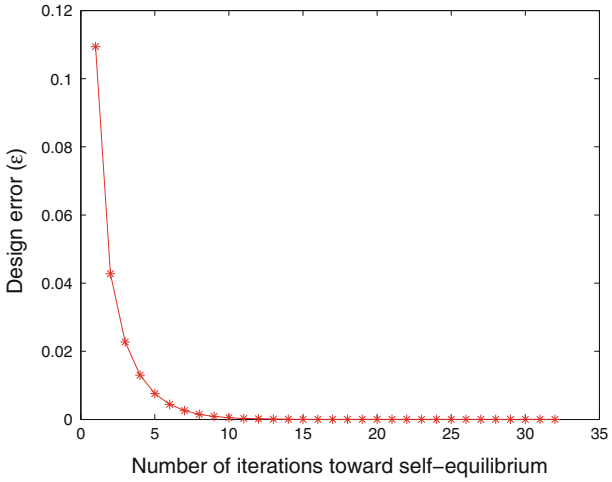

Fig. 16 The convergence of the proposed iterative algorithm for the free-form seven-strut cylindrical tensegrity structure

Table 8 The specified independent set of nodal coordinates of the seven-strut cylindrical tensegrity structure

Node	1	2	3	14
(x, y, z)	(1, 1, −1)	(−0.5, −1, 1)	(0.5, −1, −0.5)	(1, −0.5, 1)

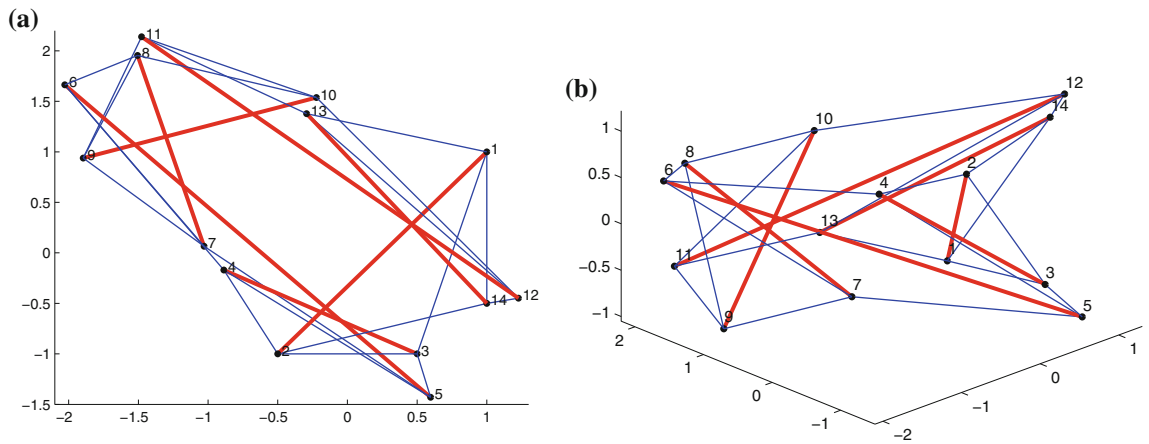

Fig. 17 The obtained free-form geometry of the seven-strut cylindrical tensegrity structure with the specified coordinates of a set of independent nodes, **a** top view, **b** perspective view

defined and shown in Fig. 17. Hence, by specifying the coordinates of a set of independent nodes, the location of some members (e.g. members 8, 15 ,16 and 22, which connect nodes 1 and 3, nodes 1 and 14, nodes 2 and 3, and nodes 1 and 2, respectively) as well as their lengths in the structure can be easily controlled.

For all mentioned examples excluding the octahedral cell, the force density matrices **D** are positive semi-definite, which lead structures to be super stable regardless of materials and prestress levels [42,46]. The stability of the octahedral cell has also been confirmed by checking the eigenvalues of its tangent stiffness matrix [31].

5 Concluding remarks

The numerical form-finding procedure of free-form tensegrity structures for both classes 1 and 2 has been presented. The topology and the initial force density vector randomly generated with the sign of each component of this vector based on the types of members are the required information. Any assumption about initial nodal coordinates or member lengths, material properties and the positive semi-definite condition of the force

density matrix is not necessary in the proposed form-finding procedure. The eigenvalue decomposition of the force density matrix and the singular value decomposition of the equilibrium matrix are performed iteratively to find the range of feasible sets of the nodal coordinates and the force densities which satisfy the required rank deficiencies of the force density and equilibrium matrices, respectively. The self-equilibrium state of free-form tensegrities can be achieved in a few of remarkable iterations. The approach of defining the unique configuration of the free-form tensegrity structure by specifying the independent set of nodal coordinates is clearly given, which implies that the geometrical and mechanical properties of the structure can be at least partly controlled by the proposed method. In the numerical examples, a very good convergence has been shown for two- and three-dimensional tensegrity structures. The proposed form-finding procedure is capable of searching new free-form configurations with limited information of the topology and the initial randomly generated force density vector.

Acknowledgments This research was supported by Basic Research Laboratory Program of the National Research Foundation of Korea (NRF) funded by the Ministry of Education, Science and Technology through NRF2010-0019373, and by Korea Ministry of Knowledge Economy under the national HRD support program for convergence information technology supervised by National IT Industry Promotion Agency through NIPA-2010-C6150-1001-0013. The authors also would like to thank the anonymous reviewers for their suggestions in improving the standard of the manuscript.

References

1. Fuller, R.B.: Synergetics-Explorations in the Geometry of Thinking. Macmillan Publishing Co. Inc., London, UK (1975)
2. Tibert, A.G., Pellegrino, S.: Deployable tensegrity reflectors for small satellites. J. Spacecr. Rocket. **39**, 701–709 (2002)
3. Fu, F.: Structural behavior and design methods of tensegrity domes. J. Constr. Steel Res. **61**, 23–35 (2005)
4. Tran, H.C., Lee, J.: Initial self-stress design of tensegrity grid structures. Comput. Struct. **88**, 558–566 (2010)
5. Kebiche, K., Kazi-Aoual, M.N., Motro, R.: Geometrical non-linear analysis of tensegrity systems. Eng. Struct. **21**, 864–876 (1999)
6. Rhode-Barbarigos, L., Ali, N.B.H., Motro, R., Smith, I.F.C.: Designing tensegrity modules for pedestrian bridges. Eng. Struct. **32**, 1158–1167 (2010)
7. Tran, H.C., Lee, J.: Self-stress design of tensegrity grid structures with exostresses. Int. J. Solids Struct. **47**, 2660–2671 (2010)
8. Ingber, D.E.: The architecture of life. Sci. Am. **278**, 48–57 (1998)
9. Ingber, D.E., Tensegrity, I.: Cell structure and hierarchical systems biology. J. Cell Sci. **116**, 1157–1173 (2003)
10. Stamenovic, D.: Effects of cytoskeletal prestress on cell rheological behavior. Acta Biomater. **1**, 255–262 (2005)
11. Connelly, R., Whiteley, W.: Second-order rigidity and prestress stability for tensegrity frameworks. SIAM J. Discret. Math. **9**, 453–491 (1996)
12. Jórdan, T., Recski, A., Szabadka, Z.: Rigid tensegrity labelings of graphs. Eur. J. Comb. **30**, 1887–1895 (2009)
13. Paul, C., Lipson, H., Valero-Cuevas, F.: Design and control of tensegrity robots for locomotion. IEEE T. Robot. **22**, 944–957 (2006)
14. Rovira, A.G., Tur, J.M.M.: Control and simulation of a tensegrity-based mobile robot. Robot. Auton. Syst. **57**, 526–535 (2009)
15. Wang, B.B.: Free-Standing Tension Structures: From Tensegrity Systems to Cable Strut Systems. Spon Press, London and New York (2004)
16. Pinaud, J.P., Solari, S., Skelton, R.E.: Deployment of a class 2 tensegrity boom. In: Proceedings of SPIE Smart Structures and Materials, pp. 155–162. (2004)
17. Lazopoulos, K.A.: Stability of an elastic tensegrity structure. Acta Mech. **179**, 1–10 (2005)
18. Lazopoulos, K.A., Lazopoulou, N.K.: On the elastica solution of a tensegrity structure: application to cell mechanics. Acta Mech. **182**, 253–263 (2006)
19. Pirentis, A.P., Lazopoulos, K.A.: On the singularities of a constrained (incompressible-like) tensegrity-cytoskeleton model under equitriaxial loading. Int. J. Solids Struct. **47**, 759–767 (2010)
20. Connelly, R., Terrell, M.: Globally rigid symmetric tensegrities. Topol. Struct. **21**, 59–78 (1995)
21. Murakami, H., Nishimura, Y.: Initial shape finding and modal analyses of cyclic right-cylindrical tensegrity modules. Comput. Struct. **79**, 891–917 (2001)
22. Sultan, C., Corless, M., Skelton, R.E.: The prestressability problem of tensegrity structures: some analytical solutions. Int. J. Solids Struct. **38**, 5223–5252 (2001)
23. Vassart, N., Motro, R.: Multiparametered formfinding method: application to tensegrity systems. Int. J. Space Struct. **14**, 147–154 (1999)
24. Schek, H.J.: The force density method for form finding and computation of general networks. Comput. Methods Appl. Mech. Eng. **3**, 115–134 (1974)
25. Motro, R., Najari, S., Jouanna, P.: Static and dynamic analysis of tensegrity systems. In: Proceedings of the International Symposium on Shell and Spatial Structures, Computational Aspects, pp. 270–279. Springer, Berlin (1986)
26. Barnes, M.R.: Form finding and analysis of tension structures by dynamic relaxation. Int. J. Space Struct. **14**, 89–104 (1999)
27. Masic, M., Skelton, R., Gill, P.: Algebraic tensegrity form-finding. Int. J. Solids Struct. **42**, 4833–4858 (2005)
28. Zhang, J.Y., Ohsaki, M.: Adaptive force density method for form-finding problem of tensegrity structures. Int. J. Solids Struct. **43**, 5658–5673 (2006)

29. Estrada, G., Bungartz, H., Mohrdieck, C.: Numerical form-finding of tensegrity structures. Int. J. Solids Struct. **43**, 6855–6868 (2006)
30. Pagitz, M., Tur, J.M.M.: Finite element based form-finding algorithm for tensegrity structures. Int. J. Solids Struct. **46**, 3235–3240 (2009)
31. Tran, H.C., Lee, J.: Advanced form-finding of tensegrity structures. Comput. Struct. **88**, 237–246 (2010)
32. Juan, S.H., Tur, J.M.M.: Tensegrity frameworks: static analysis review. Mech. Mach. Theory **43**, 859–881 (2008)
33. Sultan, C.: Tensegrity: 60 years of art, science and engineering. Adv. Appl. Mech. **43**, 69–145 (2009)
34. Tibert, A.G., Pellegrino, S.: Review of form-finding methods for tensegrity structures. Int. J. Space Struct. **18**, 209–223 (2003)
35. Zhang, L., Maurin, B., Motro, R.: Form-finding of nonregular tensegrity systems. J. Struct. Eng. ASCE **132**, 1435–1440 (2006)
36. Baudriller, H., Maurin, B., Cañadas, P., Montcourrier, P., Parmeggiani, A., Bettache, N.: Form-finding of complex tensegrity structures: application to cell cytoskeleton modelling. C. R. Mécanique **334**, 662–668 (2006)
37. Micheletti, A., Williams, W.O.: A marching procedure for form-finding for tensegrity structures. J. Mech. Mater. Struct. **2**, 101–126 (2007)
38. Rieffel, J., Valero-Cuevas, F., Lipson, H.: Automated discovery and optimization of large irregular tensegrity structures. Comput. Struct. **87**, 368–379 (2009)
39. Xu, X., Luo, Y.: Form-finding of nonregular tensegrities using a genetic algorithm. Mech. Res. Commun. **37**, 85–91 (2010)
40. Motro, R.: Tensegrity: Structural Systems for the Future. Kogan Page Science, London (2003)
41. Connelly, R.: Rigidity and energy. Invent. Math. **66**, 11–33 (1982)
42. Connelly, R.: Tensegrity structures: why are they stable? In: Thorpe, M.F., Duxbury, P.M. (eds.) Rigidity Theory and Applications, pp. 47–54. Kluwer Academic Publishers, Dordrecht (1999)
43. Calladine, C.R.: Buckminster Fuller's "tensegrity" structures and Clerk Maxwell's rules for the construction of stiff frames. Int. J. Solids Struct. **14**, 161–172 (1978)
44. Pellegrino, S., Calladine, C.R.: Matrix analysis of statically and kinematically indeterminate frameworks. Int. J. Solids Struct. **22**, 409–428 (1986)
45. Meyer, C.D.: Matrix Analysis and Applied Linear Algebra. SIAM, Philadelphia (2000)
46. Connelly, R., Back, A.: Mathematics and tensegrities. Am. Sci. **86**, 142–151 (1998)
47. Guest, S.: The stiffness of prestressed frameworks: a unifying approach. Int. J. Solids Struct. **43**, 842–854 (2006)
48. Murakami, H.: Static and dynamic analyses of tensegrity structures. Part II. Quasi-static analysis. Int. J. Solids Struct. **38**, 3615–3629 (2001)
49. Ohsaki, M., Zhang, J.Y.: Stability conditions of prestressed pin-jointed structures. Int. J. Nonlinear Mech. **41**, 1109–1117 (2006)
50. Pellegrino, S.: Structural computations with the singular value decomposition of the equilibrium matrix. Int. J. Solids Struct. **30**, 3025–3035 (1993)
51. Yang, W.Y., Cao, W., Chung, T.S.: Applied Numerical Methods Using Matlabs. Wiley InterScience, United States of America (2005)